

ANALYSIS OF RETINAL b-WAVE BY FOURIER TRANSFORMATION DUE TO AMMONIA EXPOSURE AND THE ROLE OF BLOOD ERYTHROCYTES

S.M. SHERIF, E.I. AMAL

Biophysics and Laser Science Unit, Research Institute of Ophthalmology, Giza, Egypt, P.O. Box 90
Tel: (+2) 35718305, Fax: (+2) 35752688, sheri_sm@yahoo.com

Abstract. Interest in Müller cell physiology dates back to 1962, where the origin of b-wave signal from the retina was proposed to be originating from Müller cells. There are diseases such as hepatic retinopathy resulted from elevated blood ammonia level. Although injuries associated with ammonia exposure are well studied, retinal injuries have not been adequately described in the literature. The aim of this work is firstly to investigate the effects of ammonia (gas or solution) on the b-wave of rats' retinae and secondly to employ Fourier transformation for the analysis of b-waves. To achieve these goals, albino rats were used where they exposed to ammonia, either *via* inhalation or instillation to the cornea. Retinal b-wave was recorded and then analyzed by Fourier transformation, taking into account the possible systemic role monitored by the erythrocytes osmotic fragility test and the hemoglobin characteristics. Our results indicate that the average b-wave can be resolved by Fourier transformation into several components that reflect the electrical/chemical coupling between Müller cells and the other retinal neurons. The recorded changes in the b-wave were influenced not only by the way of ammonia exposure, but also by ammonia induced fragile-erythrocytes.

Key words: b-wave, Müller cells, Fourier analysis, ammonia toxicity, osmotic fragility.

INTRODUCTION

In patients with liver insufficiency the blood ammonia concentration is elevated, which induces morphological, structural and functional retinal alterations referred to as hepatic retinopathy [17–22]. Occupational hazards due to ammonia exposure were increased as a consequence of different human activities and life modernization. Ammonia as a chemical compound is used as a fertilizer by agricultural workers [18]. It is the most important gas healthwise found in swine buildings because it can occur at levels high enough to be an irritant to the respiratory system [13]. Also, it is an important bulk chemical widely used in textiles, leather, plastics, pesticides, explosives, some refrigerant installations and

Received: March 2010;
in final form July 2010.

household cleaning products [6,18]. Ammonia is used as sprays in cases of criminal assault and armed robberies by the assailant as a method of causing temporary blindness [5], and can be produced due to different livestock operations [10]. The human is also a direct source of ammonia release. Blood and sweat ammonia concentration increased significantly during the incremental exercise [2].

The area burned by ammonia may vary considerably [3] and depends on various factors such as ammonia concentration, extent of exposure, duration of contact, regional properties, and time to treatment [26]. Anhydrous ammonia's affinity for mucosal surfaces commonly results in acute ocular injury presenting as uveitis, conjunctivitis, blepharospasm, and blindness, as well as ocular sequelae which include iritis, glaucoma, cataract and retinal atrophy [19]. Since the Müller cells are the main origin of the b-wave and its influencing by ammonia exposure has not been adequately described in the literature, we present in this article for the first time to our knowledge the analysis of b-wave by applying the Fourier transformation concept, and the impact of ammonia exposures on its functional characteristics with regard to the possible role of blood erythrocytes.

MATERIALS AND METHODS

EXPOSURE PROCEDURE

Albino (Wister) rats, 175 ± 25 g, were selected from the animal house facility at the Research Institute of Ophthalmology, Giza, Egypt. The research protocol was approved by the local ethical committee that applies the ARVO (The Association for Research in Vision and Ophthalmology) statements for using animals in ophthalmic and vision research. Rats were randomly divided into normal (control) and experimental groups (ammonia treatments). Six experimental groups, each composed of 15 rats (30 eye balls), were exposed to ammonia concentrations of 25, 50 or 100 ppm. Three experimental groups have inhaled ammonia vapor (INH-groups) in a specially designed chamber for one hour daily. The chamber was designed to have two parts separated by a porous stainless steel network. The lower part (10 cm height) contains 20 mL of different ammonia solutions (INH-25, INH-50 or INH-100 ppm). The glass lids of the animal's chambers have two 5 cm openings to allow for atmospheric oxygen and the excess ammonia vapor to flow freely. All these treatments were continued for one week. The other three experimental groups (TOP-groups) were subjected to ammonia solution topically *via* single instillation of 10 μ L of the different ammonia concentrations; TOP-25, TOP-50 or TOP-100 ppm to the cornea for 5 minutes. The ammonia was obtained from Bioedwic Co. (Cairo, Egypt) as a solution with concentration of 30%.

OSMOTIC FRAGILITY MEASUREMENT

The method used to test the osmotic fragility of erythrocytes was carried out as previously described using increasing concentrations of NaCl solutions [23]. As NaCl concentration decreases from isotonicity, a fraction of the erythrocytes hemolysis and solutions acquire red color, which is measured spectrophotometrically at 540 nm. Freshly heparinized rat blood (50 μ l) was mixed with 5 mL of different isotonic NaCl (0.9%) concentrations in the range 0–0.9%. The tubes were then mixed immediately by inverting them several times; care was taken to avoid the formation of foam. The suspensions were left for 30 min at room temperature, and then centrifuged for 5 minutes at 3000 rpm. The resultant supernatants were removed and the absorbance was estimated using Shimadzu uv-vis spectrometer (540a, Japan). Plotting the absorbance against NaCl concentrations resulted in a sigmoidal shape that is by differentiation yielding a Gaussian peak where the maximum value of this peak is known as the average osmotic fragility (H_{50}). H_{50} is the NaCl concentration producing 50% hemolysis.

HEMOGLOBIN EXTRACTION AND UV-VIS CHARACTERIZATION

Based on the procedure previously described by Trivelli *et al.* [27], heparinized blood samples were centrifuged at 1500 rpm for 10 min at 4 °C. The supernatant and the buffy coat were removed; the remaining packed cells were washed with two volumes of physiological saline (0.9% NaCl). This procedure was repeated two additional times, where the saline was removed after each washing. Packed erythrocytes were lysed with de-ionized water, and the mixture was centrifuged at 10000 rpm for 30 min at 4 °C in order to obtain hemoglobin. The absorption spectra of different hemoglobin samples were recorded in the UV-visible range 190–700 nm using Shimadzu UV-vis 240a spectrometer (Japan).

RECORDING OF RETINAL b-WAVE

The animals were dark adapted for 3 hours before the electrophysiological recording. They were anesthetized intraperitoneally by 35 mg/kg sodium thiopental, and after establishing the anesthesia, animals were placed on the pad of an operating table where their body temperature was maintained at 37 °C. Each rat was positioned with its head resting to one side and local anesthetizing eye drops were also applied. The electroretinogram (ERG) was recorded by using three Ag-AgCl electrodes. The active electrode was a wick electrode placed at the corneal periphery. The other two electrodes were placed on the skin of the lower eyelid and on the ear, as reference and earthed electrodes, respectively. A white flash was used in this work with fixed intensity (4 lux) and duration (0.2 s). The resulted electrophysiological signals were pre-amplified using CEPTU preamplifier

(Bioscience, UK). The pre-amplified signals were delivered to a computer system attached to a digital oscilloscope (Velleman Co., Taiwan), to be recorded and analyzed by the provided software.

STATISTICAL ANALYSIS

Data were expressed as the mean \pm SD. Comparison between multiple groups was performed using analysis of variance (ANOVA), commercially available statistical software package (SPSS-11, for windows) was used where the significance level was set at $p < 0.05$. All the spectral analysis was performed with OriginPro 7.5 software (Origin Lab Corporation, Northampton, MA, USA).

RESULTS

OSMOTIC FRAGILITY

The osmotic fragility data for rat erythrocytes are illustrated in Figure 1, where the normalized data are presented in panel (a). For better evaluation of these normalized curves, they were differentiated and represented in panel (b). Different parameters can be estimated from such mathematical manipulations. These parameters are: the average osmotic fragility (the peak position at x-axis, H_{50}), peak intensity and peak width as shown in Table 1. It is clear from Figure 1a that the hemolytic curves were shifted to the right side, relative to the normal, due to the inhalation of different concentrations of ammonia vapor. The average osmotic fragility as well as the corresponding peak width were increased, these changes were concomitant with a significant decrease in the peak intensities.

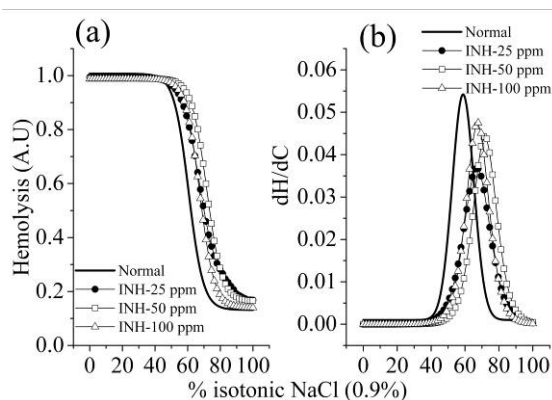


Fig. 1. Hemolytic curves in rats erythrocytes exposed to different concentrations of ammonia vapor (a), and (b) the average osmotic fragility obtained by the differentiation of curves in panel (a).

Table 1

Summary of the different parameters that resulted from the differentiation of the hemolytic curves

	Peak position (H_{50})	Peak intensity	Peak width
Normal	48 ± 0.3	0.055	10.3 ± 0.9
V-25 ppm	$\dagger 67.8 \pm 0.1$	$\dagger 0.04$	$\dagger 16.5 \pm 1.5$
V-50 ppm	$\dagger 71.2 \pm 0.6$	$\dagger 0.044$	$\dagger 15.0 \pm 1.0$
V-100 ppm	$\dagger 67.7 \pm 1.0$	$\dagger 0.048$	$\dagger 15.7 \pm 0.7$

\dagger Statistically significant.

HEMOGLOBIN CHARACTERIZATION

The UV-vis spectra, in the range 190–700 nm, of the hemoglobin molecule for the normal and ammonia treatment groups are shown in panel (a) of Figure 2. The transitions exhibited by the hemoglobin molecule in this range involve loosely bound (n or π) electrons. All the hemoglobin spectra prepared from the different ammonia vapor inhaled groups were characterized by the presence of six bands (bands 1–6) as the normal pattern. Below 200 nm, about 190 nm, the absorption band (band 1) is due to the absorption of light by the peptide bonds between the amino acid residues, which are large in number and overlap heavily, so it is difficult to resolve and assign spectral changes. In the UV range 250–300 nm (band 2), the absorption of light is due to the delocalized electrons of the aromatic side chains [11].

In the wavelength region 300 to 700 nm, the absorption of light is associated with the excitation of the porphyrin structure. The molecular orbitals involved in the electronic transitions come from the porphyrin ring, iron atom and axial ligand. The coordinated-covalent bond between iron and the proximal histidine exhibits transition at 340 nm (band 3) as previously mentioned by Ashry *et al.*, [4]. The porphyrin ring shows a characteristic intense band near 400 nm (band 4), and two additional bands near 550 nm (band 5) and 570 nm (band 6). The band near 570 nm is considered to be purely electronic transition involving the porphyrin ring of the heme group, while that near 550 nm is considered to be composed of vibronic transitions [16]. Accordingly, as shown in Table 2, each detected band has the same characteristic parameters (intensity, band width and band area) as its corresponding normal one. Moreover, the structural characteristics of Hb

molecules can be better understood by the different intensity ratios mentioned in that table. The ratio $I_{(6)/(5)}$ is larger than unity for oxygenated Hb, if there is decrease in this ratio it indicates the transformation of Hb molecule to the oxidized form which is not our case. The change in the ratios $I_{(4)/(2)}$ (increase) and $I_{(4)/(6)}$ (decrease) reflects the presence of free heme and the breakdown of Hb molecule respectively. The non-covalent bond between the heme and the protein parts was not affected as indicated by the absorbance of band (3), which implies that this bond is in its normal stretching state and did not breakdown. The second derivatives of Hb spectra shown in panel (b) were used to resolve any overlapped peaks as well as for the precise estimation of the peak positions. No change in the total number of peaks was detected.

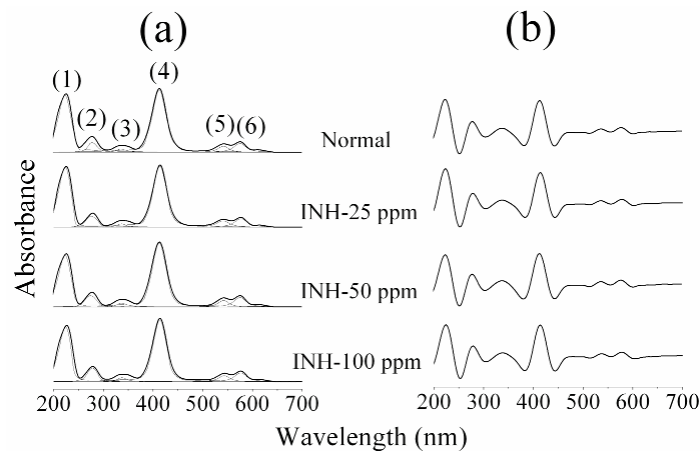


Fig. 2. UV-Visible absorption spectra of hemoglobin samples prepared from the normal and ammonia vapor treated groups (a), and their second derivative spectra (b).

ANALYSIS OF b-WAVE

Figure 3 shows the average b-wave of the different groups relative to the normal one. The useful parameters that can be used to characterize the b-wave are the amplitude, which reflects the activity of the Müller cells, and the width (time latency) that reflects the response time of the cells. In the normal b-wave, the amplitude was 0.92 ± 0.1 mV where its width was 1.8 ± 0.02 ms. Due to the inhalation of ammonia vapor there was a significant decrease in the amplitude (0.3 – 0.4 mV) associated with a significant increase in the corresponding time latency (4 – 4.5 ms). On the other hand, the same phenomena were noticed for the TOP-groups with different magnitudes; the amplitude range was 0.4 – 0.7 mV and the time latency was 2.9 – 3.9 ms.

Table 2

Summary of the hemoglobin characteristic bands and the different intensity ratios

ppm	Band (1)	Band (2)	Band (3)	Band (4)	Band (5)	Band (6)	$\ddagger I_{(4)/(2)}$	$\ddagger I_{(4)/(6)}$	$\ddagger I_{(6)/(5)}$
Normal	*27.3±1.5	14.0±4.6	14.1±4.9	28.5±1.3	20.7±3.4	24.6±1.5	4.0±0.3	6±0.5	1.3±0.3
	†36±1.7	3.9±1.0	1.3±0.9	41±1.3	3.1±1.7	5.2±1.9			
INH-25	*26.6±1.4	11.9±6.5	14.8±5.4	28±1.4	23.1±5.5	24.2±1.5	4.4±0.4	6.3±0.1	1.2±0.4
	†37.2±1.4	2.2±0.5	1.3±1.0	39.2±1.4	3.3±1.9	4.7±2.0			
INH-50	*26.8±1.6	12.2±4.5	14.0±3.8	29.5±1.3	20.1±2.4	23.8±4.6	4.6±0.4	6.0±0.2	1.3±0.1
	†32.4±1.4	3.3±0.9	1.4±0.93	43.4±1.4	3.2±1.7	5.4±1.9			
INH-100	*26.7±1.5	13.4±4.5	15.6±3.5	28.3±1.3	21.6±2.3	24.2±1.2	4.1±0.2	6.0±0.3	1.3±0.2
	†34.2±1.4	3.6±0.9	1.6±1.0	40.3±1.3	3.2±1.9	5.1±1.9			

* First line in each cell reflects the band width ± S.D.

† Second line in each cell reflects the area of the band ± S.D.

‡ Intensity ratio of the bands.

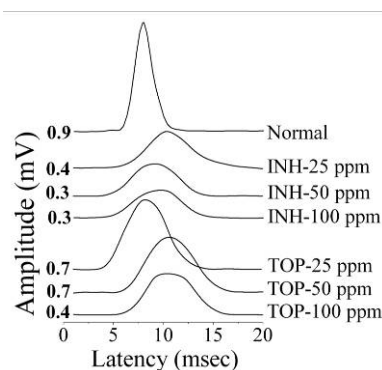


Fig. 3. Typical b-waves trace for normal and different ammonia treatment groups.

Fourier transformation is widely used in spectroscopy, particularly FTIR. With Fourier transformation, it is possible to monitor changes in the structure and properties of biomolecules such as DNA, RNA, proteins, carbohydrates, lipids in biological tissues and cell, simultaneously. Fourier transform (Figure 4) with fourth derivative, deconvolution and non-linear curve fitting methods were used to analyze b-wave signals from the Müller cells of the various animal groups used in this study. As illustrated in Figure 3, the average peak of the normal b-wave can be resolved by the curve enhancement procedure into three components with specific intensity (i.e. amplitude), peak width and peak area that are shown in Table 3. The b-wave of the INH-25 ppm and INH-50 ppm was characterized by three components too but with different amplitudes, peak widths and peak areas. As the inhaled ammonia concentration increased to 100 ppm, the average b-wave indicates the presence of four components. On the other hand, the TOP-groups

show another behavior where the number of the estimated components was three for the TOP-25 ppm, and then it increased into four components for the TOP-50 ppm and TOP-100 ppm groups. Again the relative distribution of these estimated components was differing from that of the INH-groups. The number of the estimated peaks was confirmed by the fourth derivatives shown in Figure 4.

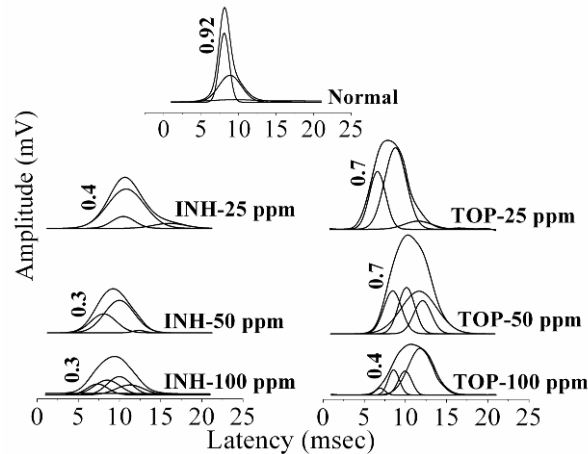


Fig. 4. Fourier deconvolution of the recorded b-waves for all studied groups and the different coupling components that resulted from the curve enhancement procedure.

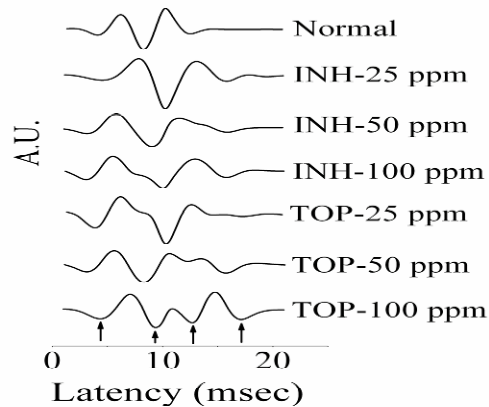


Fig. 5. Fourth derivative of the average b-waves used to confirm the number of estimated coupling components.

As shown in Table 3, these estimated components were named as comp 1–4. The detailed analysis of these components indicates that component 1 amplitude was decreased for all ammonia treatment groups, while its width increased for all ammonia exposure groups but TOP-100 ppm. On the other hand, the area under the

estimated peaks was found to be decreased in all ammonia exposed groups but TOP-25 ppm, thus mimicking the normal value of this peak. Considering component 2, the decreased amplitude was established only for INH-50 ppm and INH-100 ppm, while it fluctuated for TOP-groups, i.e., suddenly increased at TOP-25 ppm and then mimicking the normal at TOP-50 ppm, finally it decreased for the TOP-100 ppm group. The width of this component shows different characteristics; unchanged for INH-groups, and decreased for TOP-groups with the maximum decrease noticed at TOP-100 ppm group. Looking to the area, it is not changed at INH-25 ppm or INH-50 ppm, but decreased for the higher INH-ammonia concentration; 100 ppm. Regarding the peak area of the TOP-groups, it was found to be increased for TOP-25 ppm and TOP-50 ppm groups, while decreased at TOP-100 ppm one.

Table 3

Analysis of the average b-wave by Fourier transformation for all studied groups

ppm	Amplitude (mV)	Latency (msec)	Estimated components of b-wave			
			Comp1	Comp 2	Comp 3	Comp 4
Normal	0.92±0.07	1.8±0.2	^a 0.7	0.3	0.01	
			^b 1.3±0.03	3.2±0.2	7.4±1.3	
			^c 1.1±0.06	1.0±0.07	0.35±0.1	
INH-25	†0.4±0.03	†4.31±0.4	^a 0.08	0.3	0.04	
			^b 2.8±0.6	4.5±1.1	3.9±1.5	
			^c 0.3±0.1	1.5±0.8	0.17±0.03	
INH-50	†0.3±0.02	†3.8±0.4	^a 0.13	0.22	0.02	
			^b 3.1±0.7	3.6±0.5	1.5±0.5	
			^c 0.5±0.06	1.0±0.1	0.03±0.01	
INH-100	†0.3±0.07	†4.5±0.3	^a 0.07	0.1	0.12	0.06
			^b 2.5±0.4	3.2±0.3	2.9±0.1	3.4±0.8
			^c 0.2±0.08	0.4±0.06	0.4±0.02	0.3±0.09
TOP-25	†0.7±0.07	†2.9±0.3	^a 0.42	0.59	0.06	
			^b 1.9±0.5	2.6±0.6	3.4±0.6	
			^c 1.02±0.1	1.9±0.5	0.3±0.04	
TOP-50	†0.7±0.06	†3.9±0.1	^a 0.31	0.33	0.3	0.24
			^b 2.12±0.4	2.0±0.3	4.3±0.2	2.1±0.6
			^c 0.8±0.06	0.8±0.07	1.6±0.3	0.6±0.03
TOP-100	†0.4±0.05	†3.9±0.3	^a 0.05	0.17	0.17	0.32
			^b 1.08±0.05	1.3±0.4	1.6±0.1	3.1±0.3
			^c 0.07±0.01	0.3±0.1	0.33±0.08	1.3±0.2

a) The first line in these cells indicates the intensity value of the estimated component. b) The second line in these cells indicates the width of each estimated component±SD. c) The third line in these cells indicates the area of each estimated component±SD.

† Statistically significant

The amplitude of component 3 was increased in all ammonia treatment groups associated by decreased peak width also, in all groups. The area of these estimated components fluctuated without any specific trend that could be related to the ammonia exposure way or the ammonia concentration. It was decreased for INH-25 ppm, INH-50 ppm and TOP-50 ppm groups; and none changed for the rest of the groups. Component 4 appeared after the exposure to the highest INH-ammonia concentration, INH-100 ppm. As the ammonia applied topically, this component appeared at TOP-50 ppm and TOP-100 ppm groups, with amplitude, width and area values that proportionally increased with the applied ammonia concentration.

DISCUSSION

Müller cells are distributed radially across all retinal layers [1]. Interest in their physiological properties began many years ago when Faber [14] first proposed that the b-wave of the electroretinogram (ERG) was generated by the Müller cells. They constitute an anatomical and functional link between retinal neurons and blood vessels, and support the neurons by providing neurotrophic factors and blood-derived nutrients and by removing metabolic waste. Also, they are responsible for the maintenance of the homeostasis of the retinal extracellular milieu (ions, water, neurotransmitter molecules, and pH). Recent data suggest that they may also more directly contribute to information processing in the retina *via* modulation of the light-driven activity of ganglion cells [8].

The common analysis of b-wave aims to document its amplitude and width. Here, our recent analysis brings the area of the b-wave signal into consideration. Also, analyzing the contour of the b-wave using Fourier transformation concept combined with the non-linear curve fitting aiming to resolve the complex coupling nature between Müller cells and the other retinal neurons. As previously mentioned, the b-wave amplitude is indicative for the activity of Müller cells, while its width reflects the response time of the cells. In spectroscopy, the peak area usually indicates the concentration of that compound. In this work, the area reflects the number of Müller cells which participate in such chemical / electrical and/or metabolic coupling. Each estimated component resulted from Fourier analysis indicates a change in the relative coupling of the Müller-neurons network. Considering component 2, the number of cells responsible for such coupling was oscillating up or down its normal one, and in the two groups, INH-25 ppm and INH-50 ppm, it is the same. This may reflect a transitional coupling of Müller cells according to the actual physiological situation (s).

The response time of component 3 was increased relative to its normal one. Our detailed analysis gives the impetus that this component is directly related to Müller cells since it is the only component which shows a systematic response to

ammonia exposure regardless the exposure way. Another evidence that confirms this hypothesis comes from its amplitude that reflects the activity of the cells which participated in such interaction (increased activity). The number of the cells responsible for such interaction (peak area) was fluctuated without specific trends, meaning that such fluctuations are a normal physiological response buffering the induced stress. In the same context, component 4 is sensitive to the applied ammonia concentration since it was detected at higher ammonia concentrations, which may be indicative to the detoxification capacity of Müller cells. On the other hand, the activity of Müller cells inducing component 1 was decreased for all ammonia treatment groups accompanied by delayed response time but not for TOP-100 ppm. Regarding the number of cells involved in such coupling, it was decreased too but not for the TOP-25 ppm. It should be kept in our mind that these different coupling components do not operate independently; they produce the integral-average b-wave, therefore they reflect the functional interactions between Müller cells and retinal neurons including metabolic symbiosis and the processing of visual information. Accordingly, the integral activity of Müller cells was decreased due to ammonia exposure concomitant with delayed response time.

Comparing the b-wave between the INH-groups and TOP-ones would take either the possible systemic effects as well as the possible role of the cornea into consideration. The osmotic fragility of blood erythrocytes relates to the ability of its membrane to maintain its structural integrity when exposed to an osmotic stress. The osmolality at which the cells lyse is related to their shape, deformability and surface area/volume ratio, and is dependent upon their intrinsic membrane properties [7–24]. All the inhaled ammonia concentrations induce changes in the erythrocyte membrane characteristics that resulted in fragile erythrocytes as indicated by the right-shift of the sigmoidal curves (Figure 1a); this is also confirmed by resulted Gaussian peaks shown in panel b of Figure 1, where the increased peak width (Table 1) is indicative for abnormal increase in membrane elasticity. Roper *et al.* [23] mentioned that this right-shift also means that there is change in the shape of the erythrocytes that become spherical rather than ellipsoid, which will affect (reduce) its deformability. The retina is a highly metabolic organ; the b-wave was found to be affected by blood flow through the central retinal artery in laboratory animals [9–21] or in human patients [20]. Therefore, the recorded changes in the average-b-wave as well as in the individual coupling components will be influenced by the change in the blood flow/metabolic supply due to ammonia-induced fragile erythrocytes. On the other hand, the cornea contributes to approximately 2/3 of the total refraction of the eye [12]. In a previous study by Sherif [25] on the toxic effects of ammonia (gas or liquid), there were structural changes as well as vibrational ones that include both corneal lipids and proteins, which established the indirect essential role of the corneal tissue on imperfection of the eye. Both modes of ammonia application have a dualistic effect. The recorded b-wave characteristics in the INH-mode were affected by the

systemic toxic effect as well as the corneal changes. While, in the TOP-mode, the recorded b-wave characteristic was affected directly by the corneal toxicity associated with the topical application of ammonia, and by ammonia that diffused to the anterior chamber after a few seconds of injury, because of its high lipid solubility [15].

In conclusion, this article shows the possibility of applying the Fourier theory for the analysis of retinal b-wave, and that the estimated components reflect the different coupling between the Müller cells and the other neurons. There is the possibility that the recorded changes in the b-wave influenced by the pH changes associated with ammonia exposure and in case of topical contact there is the possibility of thermal damage since ammonia interacts with tissue water *via* an exothermic reaction. Applying this analysis for diagnostic purposes required further investigations since the ERG in different species differs not only due to species differences, but also due to the difference in the relative densities of the rods and cones. The toxic effect resulted from the inhaled ammonia does not extend to hemoglobin involving only the erythrocytes membrane.

REFERENCES

1. ABUKAWA, H., M. TOMI, J. KIYOKAWA, S. HORI, T. KONDO, T. TERASAKI, K. HOSOYA, Modulation of retinal capillary endothelial cells by Müller glial cell-derived factors, *Mol. Vis.*, 2009, **15**, 451–457.
2. ALVEAR-ORDENES, I., D. GARCÍA-LÓPEZ, J.A. DE PAZ, J. GONZÁLEZ-GALLEGO, Sweat lactate, ammonia and urea in rugby players, *Int. J. Sports Med.*, 2005, **26**, 632–637.
3. AMSHEL, C.E., M.H. FEALK, B.J. PHILLIPS, D.M. CARUSO, Anhydrous ammonia burns case report and review of the literature, *Burns*, 2000, **26**, 493–497.
4. ASHRY, H.A., N.S. SELIM, A.Z. EL-BEHAY, The effect of gamma-rays on the hemoglobin of whole-body irradiated mice, *Radiat. Phys. Chem.*, 1994, **44**, 187–189.
5. BEARE, J.D.L., R.S. WILSON, R.J. MARSH, Ammonia burns of the eye: an old weapon in new hands, *Br. Med. J.*, 1988, **296**, 27.
6. BELLO, A., M.M. QUINN, M. J. PERRY, D. K. MILTON, Characterization of occupational exposures to cleaning products used for common cleaning tasks – a pilot study of hospital cleaners, *Environmental Health*, 2009, **8**, 1–11.
7. BRANTON, D.C.M., J. TYLER, Interaction of cytoskeletal proteins in human erythrocyte membrane, *Cell*, 1981, **24**, 24–32.
8. BRINGMANN A., A. REICHENBACH, Müller cells, In: *Encyclopedia of Neuroscience*, Larry R. Squire ed., Academic Press Inc., London, 2009, pp. 1083–1093.
9. BROWN, K.T., K. WATANABE, Isolation and identification of a receptor potential from the pure cone fovea of the monkey retina, *Nature*, 1962, **193**, 958–960.
10. BURKHOLDER, J.A., B. LIBRA, P. WEYER, S. HEATHCOTE, D. KOLPIN, *et al.*, Impacts of waste from concentrated animal feeding operations on water quality, *Environm Health Perspect.*, 2007, **115**, 308–312.
11. CANTOR, R.C., P.R. SCHIMMEL, Techniques for the study of biological structure and function, in: *Biophysical Chemistry*, part II, 1980, p. 361–372.

12. CARVALHO, L.A., Computer algorithm for simulation of the human optical system and contribution of the cornea to the optical imperfections of the eye, *Revista de Fisica e Instrumentacao.*, 2003, **16**, 7–17.
13. DONHAM, K.J., S.J. REYNOLDS, P. WHITTEN, J.A. MERCHANT, L. BURMEISTER, W.J. POPENDORF, Respiratory dysfunction in swine production facility workers: dose response relationships of environmental exposures and pulmonary function, *Am. J. Ind. Med.*, 1995, **27**, 405–418.
14. FABER, D.F., *Analysis of Slow Transretinal Potentials in Response to Light*, Ph.D. thesis, State University of New York at Buffalo, 1969.
15. GOOD, D.W., M. A. KNEPPER, Ammonia transport in the mammalian kidney, *Am. J. Physiol.*, 1985, **248**, F459–471.
16. GOUTERMANN, M., Optical spectra and electronic structure of porphyrins and related rings, in: *The Porphyrins*, vol. 3D, Dolphin ed., Academic Press, New York, 1978, pp. 1–156.
17. KUHRT, H., M. WALSKI, A. REICHENBACH, J. ALBRECHT, Rabbit retinal organ culture as an *in vitro* model of hepatic retinopathy, *Graefes Arch. Clin. Exp. Ophthalmol.*, 2004, **242**, 512–522.
18. LEDUC, D., P. GRIS, P. LHEUREUX, P.A. GEVENOIS, P.D. VUYST, J.C. YERNAULT, Acute and long term respiratory damage following inhalation of ammonia, *Thorax*, 1992, **47**, 755–757.
19. LEE, J.H., C.L. FARLEY, C.D. BRODRICK, P.H. BLOMQUIST, Anhydrous ammonia eye injuries associated with illicit methamphetamine production, *Ann. Emerg. Med.*, 2003, **41**, 157.
20. NILSSON, S.E., Human retinal vascular obstructions. A quantitative correlation of angiographic and electroretinographic findings, *Acta Ophthalmol.* (Copenhagen), 1971, **49**, 111–133.
21. NOELL, W.K., The origin of the electroretinogram, *Am. J. Ophthalm.*, 1954, **38**, 78–90.
22. REICHENBACH, A., U. FUCHS, M. KASPER, E. EL-HIFNAWI, A.K. ECKSTEIN, Hepatic retinopathy: morphological features of retinal glial cells accompanying hepatic failure, *Acta Neuropathol.*, 1995, **90**, 273–281.
23. ROPER, D., L. MARK, L. MITCHELL, Investigation of the hereditary haemolytic anaemia: membrane and enzyme abnormalities, in: *Dacie and Lewis Practical Haematology*, Churchill Livingstone, New York, 2001, pp. 167–173.
24. SERRANI, R.E., D. ALONSO, J.L. CORCHS, States of stability/lysis in human fetal and adults red blood cells, *Arch. Int. Physiol. Biochem.*, 1989, **97**, 309–316.
25. SHERIF, S.M., Corneal toxicity associated with ammonia exposure investigated by Fourier infrared spectroscopy, *Biophys. Rev. Letters*, 2009, **4**, 331–343.
26. SYKES, R.A., M.M. MANI, J.M. HIEBERT, Chemical burns: retrospective review, *J. Burn Care Rehabil.*, 1986, **7**, 343–347.
27. TRIVELLI, L.A., H.M. RANNEY, H.T. LAI, Hemoglobin components in patients with diabetes mellitus, *N. Engl. J. Med.*, 1971, **284**, 353–357.